

A catalogue of emission lines in spectra of Comet C/1995 O1 (Hale-Bopp)*

H. W. Zhang^{1,2,3}, G. Zhao¹, and J. Y. Hu¹

¹ Beijing Astronomical Observatory, Chinese Academy of Sciences, Beijing 100012, PR China

² Department of Astronomy, Peking University, Beijing 100871, PR China

³ Beijing Astrophysics Center, Jointly sponsored by the Chinese Academy of Sciences and Peking University, Beijing 100871, P.R. China

Received 29 June 2000 / Accepted 23 November 2000

Abstract. High-resolution and high signal-to-noise ratio spectra of Comet C/1995 O1 (Hale-Bopp), which provided continuous wavelength coverage from 5500 Å to 8500 Å and partial coverage from 4000 Å to 5500 Å, were obtained with the Coudé Echelle Spectrograph at Beijing Astronomical Observatory on March 26, 28 and April 22, 1997. In the spectra we found 532 emission features, among which 459 lines from H, O, Na, C₂, C₃, CN, CH, NH₂ and H₂O⁺ were identified. The intensity of sodium emission lines at 5890 Å and 5896 Å on April 22 increased about 5 fold compared to that recorded on March 26 and 28. The intensity ratio $I_{\lambda 5577}/(I_{\lambda 6300} + I_{\lambda 6364})$ of [O I] is consistent with the formation of excited O atoms from the photodissociation of H₂O.

Key words. comets: general – comet: C/1995 O1 (Hale-Bopp)

1. Introduction

High-resolution spectral observation of Comet C/1995 O1 (Hale-Bopp) provides an opportunity to investigate the cometary chemical composition. It is significant that comets are the least modified remnants of the creation of the solar system and can provide insight into conditions existing in the early solar system. Low resolution optical spectra of many comets have been obtained (e.g. Hicks & Fink 1996). Arpigny (1995) pointed out that some 200–300 of the approximately 2000 emission lines in the optical region of cometary spectra have yet to be assigned as molecular species.

With echelle spectrographs, we can obtain high resolution and large wavelength coverage spectra in optical regions. Such high resolution optical spectra of comets can be used to identify new molecular species. For example, Brown et al. (1996) gave a catalogue with 2997 emission lines based on high resolution spectra of comet Swift-Tuttle and Brorsen-Metcalf over the range of 3800–9000 Å. They identified 2438 lines caused by H, O, C₂, CN, NH₂, C₃, H₂O⁺, CH and CH⁺. Morrison et al.

(1997) also obtained the high resolution spectra of Comet C/1996 B2 (Hyakutake). However, some emission lines found in comets are still unidentified. Although many of the unidentified features are likely to belong to already-known radicals and ions, the existence of yet unknown molecules responsible for these emissions cannot be excluded. Therefore, it is important to verify the presence of these lines in more comets. Their variation from comet to comet might also be helpful in identification.

In this paper, we present a catalogue of emission lines from the high-resolution and high signal-to-noise ratio spectra of Comet C/1995 O1 (Hale-Bopp). The observation and data reduction are described in Sect. 2. The line identifications are described in Sect. 3. A brief discussion of our results on Na and [O I] is given in Sect. 4.

2. Observation and data reduction

The observation was made by using the Coudé Echelle Spectrograph mounted on the 2.16 m telescope at Beijing Astronomical Observatory (Xinglong, China). The detector was a Tek CCD (1024 × 1024 pixels of 24 μm × 24 μm each). The Coudé Echelle Spectrograph consists of a blue path and a red path. For the blue path, the 79 grooves/mm echelle grating was used, along with a prism as cross disperser and a 0.5 mm (1.06'') slit leading to a resolving power of the order of 44000. For the red path, the 31.6 grooves/mm echelle grating was used, along with a

Send offprint requests to: H. W. Zhang,
e-mail: zhw@bac.pku.edu.cn

* Table 3 is only available in electronic form at the CDS via anonymous ftp to cdsarc.u-strasbg.fr (130.79.128.5) or via <http://cdsweb.u-strasbg.fr/cgi-bin/qcat?J/A+A/367/1049>

Table 1. Journal of observations. The observation date, the universal time of mid-exposure, the exposure duration, the signal-to-noise ratio on continuum at 6400 Å, the spectrum range, the geocentric and heliocentric distances (Δ , r) and the radial velocities ($\dot{\Delta}$, \dot{r}) of the comet interpolated to the time of mid-exposure are listed. The ephemeris for Comet C/1995 O1 (Hale-Bopp) was computed from the orbit solution #55 published on March 4, 1997 by Yeomans and are available to the public via Internet (<http://encke.jpl.nasa.gov/eph.html>)

Date	U.T.	Exp. Time (min)	S/N (pixel ⁻¹)	Sp. Range	Δ (AU)	r (AU)	$\dot{\Delta}$ (km s ⁻¹)	\dot{r} (km s ⁻¹)
26/03/1997	11:22:45	30	180	Red	1.322	0.920	5.6	-3.5
28/03/1997	11:45:42	20	180	Red	1.330	0.918	8.3	-1.8
28/03/1997	12:09:54	20	280	Red	1.330	0.918	8.3	-1.8
22/04/1997	11:47:55	20	80	Blue	1.627	0.991	28.4	12.2

prism as cross disperser and a 0.5 mm (1.06") slit leading to a resolving power of the order of 37 000. The wavelength coverage in one exposure is limited by CCD size.

The spectra of Comet C/1995 O1 (Hale-Bopp) were obtained on March 26, 28 and April 22, 1997 (see Table 1). The slit was positioned on the brightest point of the comet and manually guided on the comet. Four spectra were obtained during these observations. They provided continuous wavelength coverage from 5500 Å to 8500 Å and partial coverage from 4000 Å to 5500 Å. The wavelength coverage of each spectrum is listed in Table 2. The spectrum of the moon was observed on March 27.

The spectra were reduced with the ESO MIDAS package on a SUN Sparc 20 workstation at Beijing Astronomical Observatory (Beijing, China). The data reduction includes locating the echelle order on the multi-order two dimensional spectrum, subtracting the background, and extracting the orders by summation along the slit. The pixel-to-pixel variation was corrected by dividing by flat fields taken at the same night. The wavelength calibration was based on a thorium-argon lamp. The continuum level was determined by fitting a spline curve to a set of continuum window (typically 20–30 per order). The continuum windows of spectra were selected by inspection of the solar atlas (Moore et al. 1966). The ranges of cometary emissions were excluded by checking sudden variations in intensity compared to intensities in neighbouring continuum windows. Division of the spectrum by the fitted curve yielded a normalized spectrum. Since the conditions were not photometric in both March and April, no accurate absolute calibration could be made. The spectral atlas with the wavelength range from 5500 Å to 8500 Å of Comet C/1995 O1 (Hale-Bopp) on 28 March was published by Zhang et al. (1997a,b).

3. Line identification

In order to distinguish emission features, moon spectra were subtracted. Both comet and moon spectra were shifted to the continuum at zero heliocentric radial velocity. A portion of the subtracted spectra on March 28 is shown in Fig. 1.

Emission features were searched for in all subtracted spectra, and every feature was cross-checked in several

spectra covering the same wavelength range. Emission lines between 5500 Å to 8500 Å, which were confirmed in different spectra, were included in our line catalogue. In addition, very strong and significant emission lines between 4000 Å and 5500 Å were selected. Regions around 6900 Å and 7600 Å in which water lines are rich were skipped because of spurious emission features at the locations of water lines in the subtracted spectra. In order to exclude the residuals of the continuum subtraction, the emission features were also checked in the unnormalized and unsubtracted spectra. Emission lines from the sky, primarily due to OH, were identified and removed using the table of Osterbrock et al. (1996). The wavelengths and equivalent widths (EW s) of emission features were measured. The accuracy of the wavelength measurement is about 0.1 Å. Finally, 532 secure emission features were selected for our line catalogue. Weak features ($EW < 5$ mÅ) were excluded.

Our line identifications are based on wavelength coincidences only. The catalogue of Brown et al. (1996) was used as a starting line list. In total, we identified 459 of 532 emission features, which included 231 C₂ lines, 163 NH₂ lines, 45 CN lines, 6 H₂O⁺ lines, 7 CH lines, 1 C₃ lines, 3 [O I] lines, 2 Na lines and 1 H line. Table 3 lists all of the lines found in spectra and their identifications, if known. An example of Table 3 is given here. The complete catalogue is provided only in electronic form at the CDS. Table 4 lists all 73 unidentified lines.

Figure 2 gives, in graphical form, the average wavelengths and EW s of cometary emission lines between 5500 Å and 8500 Å. The figure shows that NH₂ lines are relatively strong and C₂, CN, and H₂O⁺ lines are quite weak. Probably, the reason is the differences in abundances and spatial distribution of the species in the comet.

Compared with Fig. 1b of Brown et al. (1996) and Fig. 1 of Morrison et al. (1997), Fig. 1a of this paper shows that NH₂ and some unidentified lines are significantly stronger, relative to the C₂ lines. This may be a clue to the origin of the unidentified lines. Considering wavelengths and relative strengths, we suspect that these unidentified lines are NH₂ lines. However, the identification of these lines will be the subject of our forthcoming work.

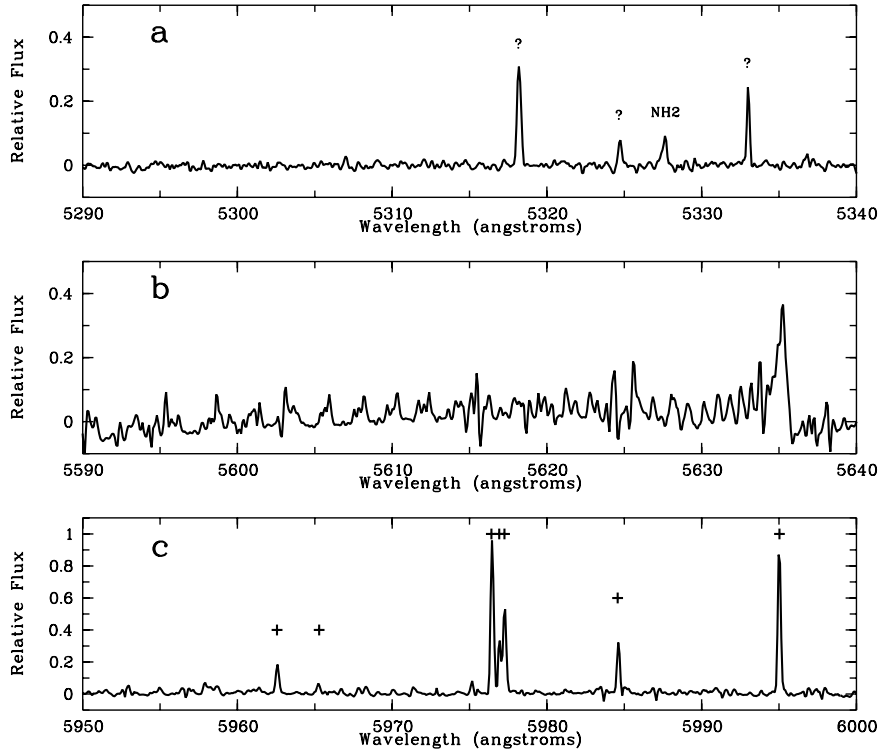


Fig. 1. A portion of comet spectra. **a)** A region showing unidentified lines marked with “?”. **b)** A region showing the C₂ band. **c)** A region showing NH₂ lines marked with a cross

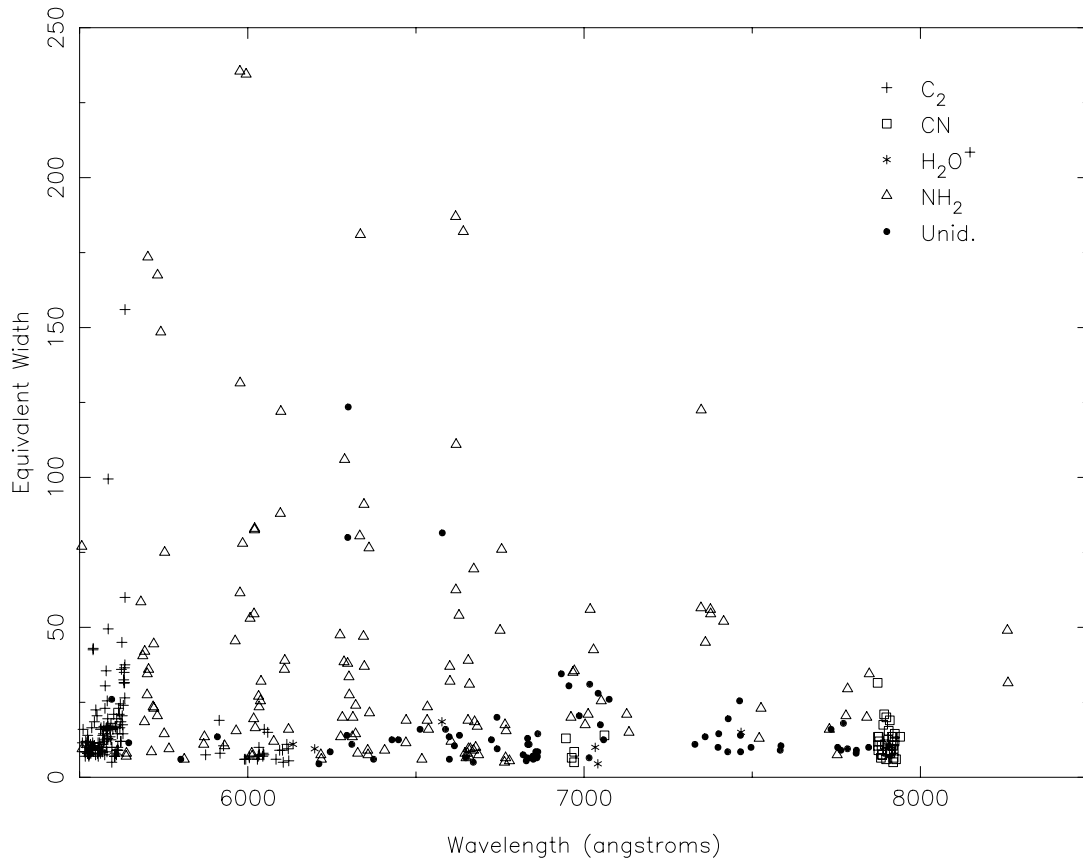


Fig. 2. Emission lines found in spectra between 5500 Å and 8500 Å; unit of equivalent width is mÅ

Table 2. Wavelength coverage of the echelle spectra

Echelle order	26 March	28 March	28 March	Echelle order	22 April
66	8498-8617			35	6344-6423
67	8372-8489	8406-8521	8456-8577	36	6168-6245
68	8248-8364	8283-8396	8330-8450	37	6001-6076
69	8127-8240	8162-8276	8208-8325	38	5843-5916
70	8013-8125	8046-8157	8089-8204	39	5693-5765
71	7898-8011	7933-8042	7973-8087	40	5551-5620
72	7790-7900	7823-7930	7861-7974	41	5416-5483
73	7684-7791	7715-7822	7752-7863	42	5287-5353
74	7580-7686	7611-7716	7646-7755	43	5164-5228
75	7480-7584	7510-7613	7543-7651	44	5046-5109
76	7381-7484	7411-7513	7442-7549	45	4934-4996
77	7286-7387	7315-7416	7345-7449	46	4827-4887
78	7192-7292	7221-7321	7250-7353	47	4724-4783
79	7101-7200	7130-7228	7157-7259	48	4626-4684
80	7012-7110	7041-7138	7066-7167	49	4532-4588
81	6926-7023	6954-7050	6978-7077	50	4441-4496
82	6842-6937	6870-6964	6892-6990	51	4353-4408
83	6760-6854	6787-6880	6808-6905	52	4270-4323
84	6679-6772	6706-6798	6726-6822	53	4189-4241
85	6601-6693	6628-6719	6646-6741	54	4111-4163
86	6524-6615	6551-6640	6568-6662	55	4037-4087
87	6449-6539	6476-6564	6491-6584	56	3965-4015
88	6376-6465	6402-6490	6417-6509		
89	6304-6392	6330-6417	6345-6435		
90	6234-6321	6260-6346	6273-6363		
91	6166-6252	6191-6276	6204-6292		
92	6099-6184	6124-6208	6135-6223		
93	6034-6118	6058-6141	6069-6155		
94	5970-6053	5994-6076	6004-6089		
95	5907-5989	5931-6012	5940-6025		
96	5845-5927	5869-5950	5878-5961		
97	5785-5866	5809-5888	5816-5899		
98	5727-5806	5750-5829	5757-5839		
99	5669-5747	5692-5769	5698-5779		
100	5612-5690	5635-5712	5641-5721		
101	5557-5634	5579-5656	5585-5664		
102	5502-5579	5525-5600	5529-5608		
103	5471-5546	5475-5553			

4. Discussion

4.1. Na

The velocities and equivalent widths of sodium *D* emission lines on March 26, 28 and April 22 were measured (see Table 5). Compared with the geocentric radial velocities of the comet, Δ , see Table 1, the nucleocentric velocities are small, less than the error of measurement. The small nucleocentric velocities are expected since the slit was positioned at the center of brightness of the comet.

The sodium emission feature of comets is caused by resonant scattering of the incoming solar light. Therefore, the line intensity and acceleration of sodium atoms by solar radiation pressure depends strongly on the Doppler shift with respect to the solar Fraunhofer absorption lines (Swings effect). Figure 3 shows the comparison of sodium emissions from spectra taken on March 26, 28 and April 22. The intensity of sodium emission lines on April 22 increases about 5 times compared to March 26, 28, because the solar flux at the excitation wavelength of

Table 3. A sample of the catalogue of emission lines. In the table, Cols. 1–6 give wavelengths and EW s of emission features on March 26, 28 and April 22, respectively. Columns 7–10 list the laboratory wavelengths of given identification, identified species, bands and transitions, respectively. If the emission features are blended by two or more lines, identified molecules, bands and transitions are listed in subsequent rows. If the emission line is unidentified, Col. 8 states “unid.”

λ_{26} (Å)	EW_{26} (mÅ)	λ_{28} (Å)	EW_{28} (mÅ)	λ_{22} (Å)	EW_{22} (mÅ)	λ_{lab} (Å)	Species	Band	Transition
5811.29	6	5811.34	6			5811.28	NH ₂	(0,10,0)	3 ₃₀ –2 ₂₀
5868.87	11	5868.80	11	5868.83	7	5868.82	NH ₂	(1,6,0)	3 ₃₀ –4 ₄₀
5871.00	11	5871.09	16	5871.07	17	5871.04	NH ₂	(1,6,0)	3 ₃₀ –4 ₄₀
5874.54	8	5874.58	7			5874.49	C ₂	(1,3)	$R_1(57)+R_2(56)+R_3(55)$
						5874.50	C ₂	(3,5)	$R_3(38)$
5890.00	260	5889.97	262	5889.95	1412	5889.97	NaI		
5896.01	240	5896.00	170	5895.95	774	5895.94	NaI		
5909.70	14	5909.68	13	5909.63	11		unid.		
5915.12	18	5915.13	20	5915.15	21	5915.23	C ₂	(3,5)	$R_1(31)+R_2(30)$
5917.73	10	5917.68	6			5917.76	C ₂	(2,4)	$R_1(41)$
						5917.68	C ₂	(5,7)	$P_1(24)$
5927.99	7	5928.05	14			5928.06	C ₂	(2,4)	$R_1(39)$
5931.06	9	5931.02	12			5931.07	NH ₂	(1,10,0)	2 ₂₀ –1 ₁₁
5962.68	43	5962.56	48			5962.61	NH ₂	(0,9,0)	3 ₀₃ –2 ₁₁
						5962.54	NH ₂	(0,9,0)	3 ₀₃ –2 ₁₁
5965.27	14	5965.28	17			5965.19	NH ₂	(0,9,0)	2 ₀₂ –1 ₁₀
5976.49	223	5976.41	248			5976.40	NH ₂	(0,9,0)	1 ₀₁ –1 ₁₁
						5976.50	NH ₂	(0,9,0)	1 ₀₁ –1 ₁₁

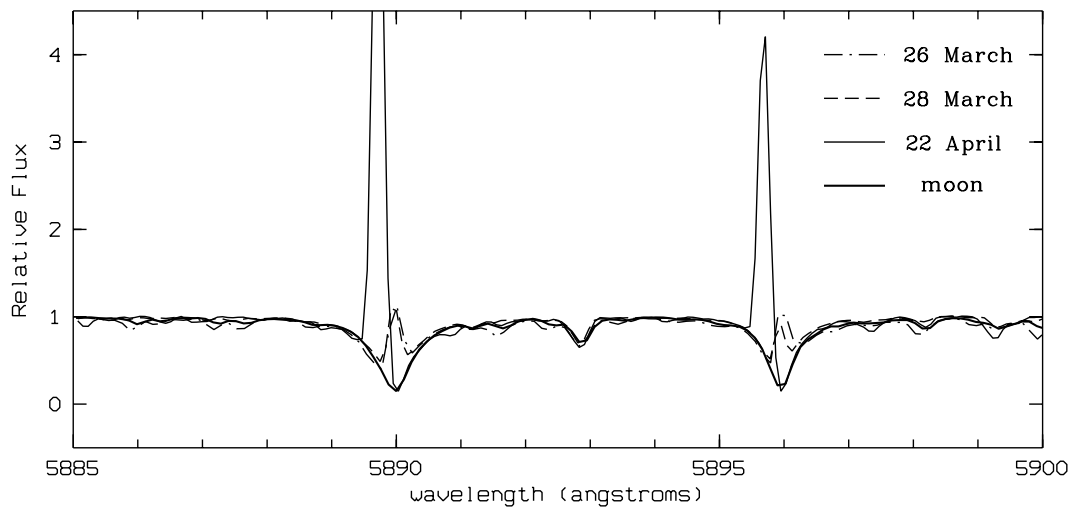


Fig. 3. Comparison of sodium emission on 26, 28 March and 22 April. The cometary continuum is shifted to zero-velocity position. The moon spectrum is also drawn as a reference with the Na D Fraunhofer line

the cometary sodium lines on April 22 is higher than on March 26, 28.

According to calculations of Arpigny et al. (1998), our Na D_2/D_1 ratio agrees with the model combining resonance scattering and telluric water lines (case 2 in Arpigny et al. 1998). It supports the results of Arpigny et al. (1998).

4.2. [OI]

The spectra include $\lambda 5577$ ($^1S - ^1D$) and the red doublet $\lambda\lambda 6300, 6364$ ($^1D - ^3P$) of [O I]. The intensity ratio, $I_{\lambda 5577}/(I_{\lambda 6300} + I_{\lambda 6364})$, is used to determine the parent

molecule which dissociates and forms the excited O atoms. In particular, the dissociation of H₂O produces roughly ten times as many atoms in the 1D as in the 1S state and leads to an intensity ratio around 0.10 (Festou et al. 1981). On the other hand, the dissociation of pure CO₂ or CO leads to roughly equal populations in the two states and, to some extent, it contributes to the production of O with a large intensity ratio. Morrison et al. (1997) and Fink & Johnson (1984) found that the data are well explained by the dissociation of H₂O alone.

The average EW s for $\lambda\lambda 5577, 6300$ and 6364 are 0.032, 0.123 and 0.041 Å, respectively. If the blends with

Table 4. Unidentified lines. In the table, Cols. 1–5 and 6 give wavelengths and *EW*s of emission features on March 22, 28 and April 22 respectively, Cols. 7 and 8 give wavelengths and relative intensities listed by Brown et al. (1996). Columns 9 and 10 give wavelengths and *EW*s listed by Morrison et al. (1997)

λ_{26} (Å)	<i>EW</i> ₂₆ (mÅ)	λ_{28} (Å)	<i>EW</i> ₂₈ (mÅ)	λ_{22} (Å)	<i>EW</i> ₂₂ (mÅ)	λ_B (Å)	<i>I</i> _B (Rel.)	λ_M (Å)	<i>EW</i> _M (mÅ)
				4838.27	36	4838.20	19		
				4838.53	36	4838.40	58		
				4850.66	16	4850.62	22		
				5306.98	9	5306.91	50		
				5318.19	98	5318.15	172	5318.079	381
				5333.01	65	5333.04	103	5332.924	212
				5428.19	24	5428.15	110		
5586.15	17	5586.22	16	5586.27	21	5586.18	98	5586.181	99
5595.35	25	5595.36	27	5595.39	32	5595.36	59	5595.322	101
5646.08	15	5646.10	8			5646.06	35		
5800.90	7	5800.89	5			5800.75	35		
5909.70	14	5909.68	13	5909.63	11			5909.640	81
6245.17	8	6245.10	9			6245.05	113		
6294.85	17	6294.82	11			6294.83	58		
6297.33	78	6297.37	82			6297.17	551		
6298.75	119	6298.65	128			6298.66	484		
6309.60	14	6309.44	8			6309.46	111		
6374.16	6	6374.04	6	6374.27	7	6374.15	41		
6428.80	14	6428.78	11			6428.74	56		
6448.15	13	6448.08	12			6448.04	107		
6512.46	8	6512.33	24			6512.37	66		
6578.19	82	6578.21	81			6578.11	130		
6588.10	16	6587.99	16			6588.01	68	6587.928	66
6598.84	15	6598.78	12			6598.83	110		
6599.43	5	6599.38	8			6599.26	51		
6614.41	10	6614.46	11			6614.39	46		
6629.52	18	6629.55	10			6629.50	45		
6647.92	6	6647.91	7			6647.89	50		
6670.58	5	6670.61	6			6670.53	47		
6724.39	13	6724.41	12			6724.42	40		
6740.91	20	6740.82	20			6740.83	67	6740.803	55
6741.73	9	6741.58	10			6741.60	55		
6818.85	7	6818.78	8			6818.75	47		
6828.11	6	6828.03	5			6827.99	50		
6830.94	7	6830.86	6			6830.87	45		
6831.89	12	6831.85	14			6831.84	129		
6832.48	11	6832.45	11			6832.48	48		
6836.61	11	6836.53	11			6836.47	118		
6847.34	7	6847.32	7			6847.22	47		
6848.64	5	6848.68	8			6848.59	59		
6856.08	10	6856.16	16			6856.09	44		
6859.38	7	6859.39	6			6859.31	47		
6860.91	8	6860.84	6			6860.81	40		
6862.20	14	6862.18	15			6862.08	54		
6862.45	8	6862.39	9			6862.31	61		
6932.30	34	6932.32	35			6932.32	192		
6954.84	36	6954.76	25			6954.77	78		
6985.52	22	6985.53	19			6985.51	81		
7014.67	7	7014.77	6			7014.68	41		
7016.67	20	7016.56	42			7016.63	126		
7041.81	18	7041.72	38			7041.68	66		
7048.30	16	7048.26	19			7048.22	52		
7058.21	9	7058.21	16			7058.09	39		
7074.38	27	7074.40	25			7074.36	64		
7329.49	10	7329.53	12			7329.48	40		
7359.70	12	7359.70	15			7359.70	61		
7398.17	7	7398.12	13			7398.06	44		
7400.29	11	7400.42	18			7400.42	51		
7426.96	9	7426.94	8			7426.83	40		
7428.38	21	7428.47	18			7428.42	52		
7464.84	15	7464.68	13			7464.68	106		
7465.31	10	7465.44	7			7465.37	50		
7496.34	11	7496.30	9			7496.23	33		
7583.07	10	7583.00	8			7583.00	35		
7585.31	10	7585.29	11			7585.30	36		
7734.11	16	7733.96	16			7733.96	40		
7753.70	9	7753.76	11			7753.64	40		
7763.50	9	7763.45	9			7763.47	39		
7771.05	19	7771.02	17			7770.97	109		
7783.08	10	7783.09	9			7783.03	35		
7808.81	10	7808.84	6			7808.73	24		
7809.63	8	7809.61	10			7809.62	29		
7846.10	8	7846.07	12			7846.10	41		

Table 5. Results of sodium emission lines. The velocities and equivalent width ratio D_2/D_1 of emission lines are listed

Date	Nucleocentric velocities (km s^{-1})	D_2/D_1
26 March	-0.5	1.08
28 March	-0.8	1.54
22 April	-2.5	1.82

C_2 lines at 5577.40 \AA and 5577.54 \AA are considered, the equivalent width for $\lambda 5577$ ($^1\text{S} - ^1\text{D}$) is $0.026 \pm 0.003 \text{ \AA}$.

We corrected the ratio of normalized line fluxes for the slope of the solar continuous flux, which we took from Allen (1973). The slope of the reflectance spectrum of the comet is unknown. With a wavelength-independent reflectance, the [OI] intensity ratio $I_{\lambda 5577}/(I_{\lambda 6300} + I_{\lambda 6364})$ is 0.22 or 0.18 with the correction for blending of $\lambda 5577$. The ratio is consistent with the production of O atoms by the dissociation of H_2O , according to the model by Festou et al. (1981).

Acknowledgements. We are grateful to the referee for very helpful comments. We also thank Mr. H. B. Li for his help during the observation and data reduction. The research work

is supported by the National Natural Science Foundation of China under grant 19725312 and NKBRSF No. G1999075406.

References

- Allen, C. W. 1973, *Astrophysical Quantities*, 3rd edition (London, Athlone Press), 172
- Arpigny, C., Rauer, H., Manfroid, J., et al. 1998, *A&A*, 334, L53
- Arpigny, C. 1995, in *Laboratory and Astronomical High Resolution Spectra*, ASP Conf. Ser., 81, 362
- Arpigny, C. 1994, in *50th International Meeting of Physical Chemistry*, AIP Conf. Proc., No. 50 (AIP, New York)
- Brown, M. E., Bouchez, A. H., Spinrad, H., et al. 1996, *AJ*, 112, 1197
- Festou, M. C., Rickman, H., & West, R. M. 1993, *ARA&A*, 5, 37
- Festou, M. C., & Feldman, P. D. 1981, *A&A*, 103, 154
- Fink, U., & Johnson, J. R. 1984, *AJ*, 89, 1565
- Hicks, M. D., & Fink, U. 1996, *ApJ*, 459, 729
- Moore, C. E., Minnaert, M. G. J., & Houtgast, J. 1966, *The Solar Spectrum 2935 \AA to 8770 \AA*, National Bureau of Standards Monograph 61, Washington
- Morrison, N. D., Knauth, D. C., Mulliss, C. L., et al. 1997, *PASP*, 109, 676
- Osterbrock, D. E., Fullbright, J. P., Martel, A. R., et al. 1996, *PASP*, 108, 277